Supplemental Information

The inhibitory receptor NKG2A sustains virus-specific $CD8^+$ T cells in response to a lethal poxvirus infection

Aaron S. Rapaport, Jill Schriewer, Susan Gilfillan, Edward Hembrador, Ryan Crump, Beatrice F. Plougastel, Yaming Wang, Gaelle Le Friec, Jian Gao, Marina Cella, Hanspeter Pircher, Wayne M. Yokoyama, Mark R. Buller, Marco Colonna.

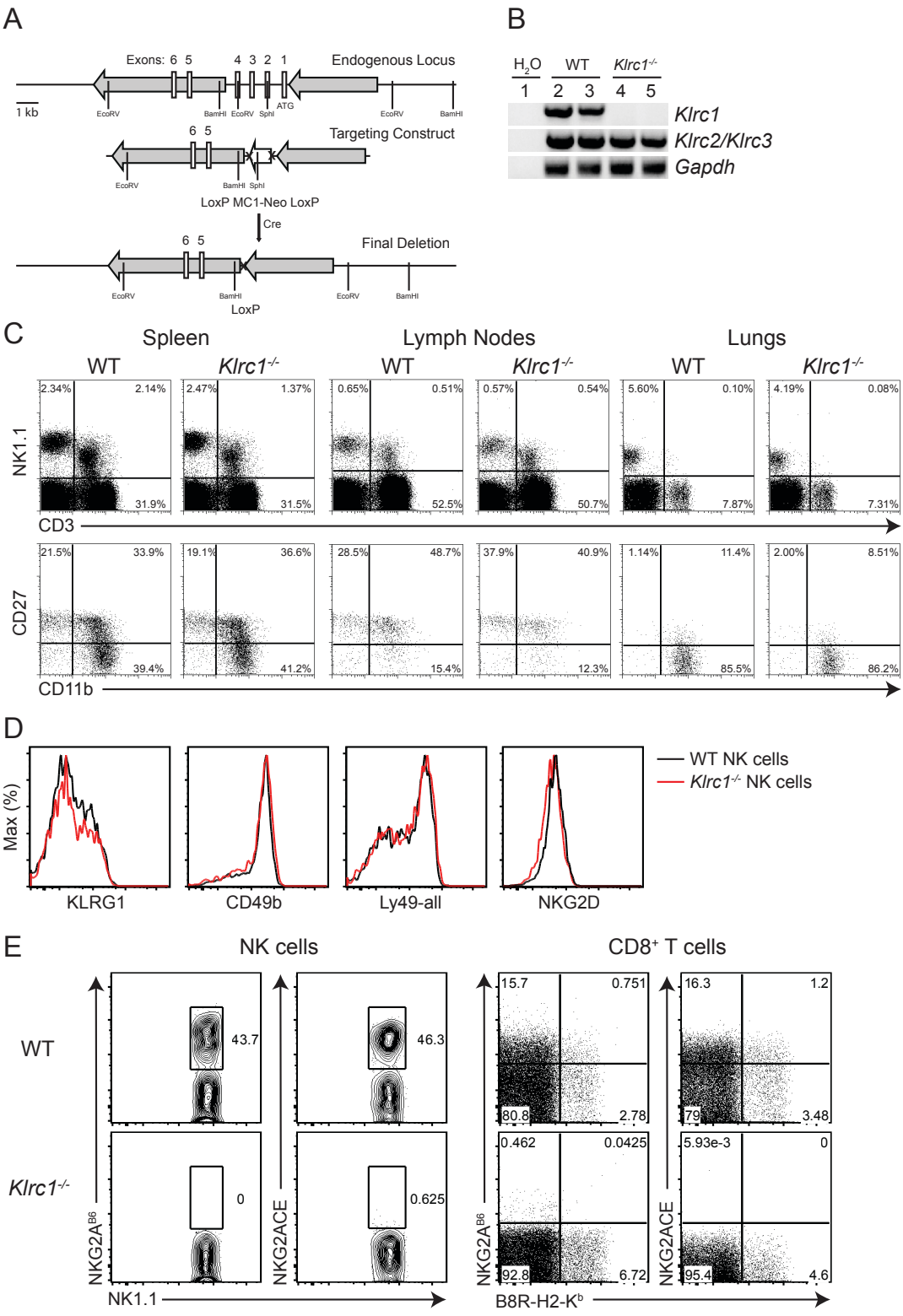

Supplemental Figure 1, related to Figure 1: Generation and characterization of *Klrc1*$^{-/-}$ mice. (**A**) Schematic representation of *Klrc1*-knockout targeting. A targeting vector that would replace the first four exons of

the *Klrc1* genomic locus was tranfected into the *B6*^{blu} embryonic stem cell line. One of the 209 clones integrated properly, as judged by southern blot screening, and was injected into C57BL/6 blastocysts. Mice heterozygous for the *Klrc1* deletion were successfully bred from the chimeric mice. Heterozygote crosses resulted in the breeding of *Klrc1*$^{-/-}$ mice, which were born at Mendelian ratios and developed normally. (**B**) RNA was isolated from WT and *Klrc1*$^{-/-}$ splenocytes and *Klrc1*, *Klrc2/Klrc3*, and *Gapdh* mRNA expression was visualized by cDNA synthesis followed by PCR amplification. Lane 1 represents water input negative controls, lanes 2 and 3 are naïve WT cDNA samples, and lanes 4 and 5 are naïve *Klrc1*$^{-/-}$ cDNA samples. (**C**) T cell and NK cell frequencies were assessed in spleens, mesenteric lymph nodes, and lungs (top row). Peripheral NK cell populations were assessed for maturation markers CD11b and CD27 in the same tissues (bottom row). (**D**) Expression of representative NK cell surface receptors KLRG1, CD49b, Ly49 family, and NKG2D was assessed on naïve splenic NK cells. (**E**) Comparison of anti-NKG2ACE and anti-NKG2A^{B6} staining on both WT and *Klrc1*$^{-/-}$ NK cells and activated CD8^{+} T cells.

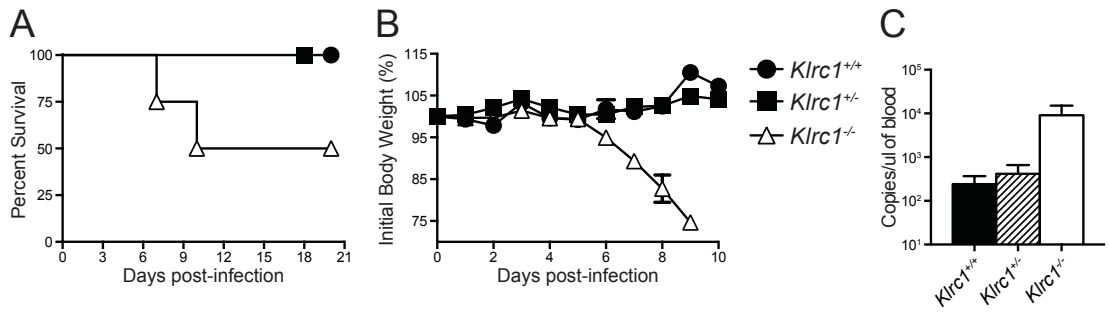

Supplemental Figure 2, related to Figure 2: Susceptibility to ECTV segregates with the targeted mutation of *Klrc1*. *Klrc1*$^{-/-}$ mice were backcrossed to WT C57BL/6 mice and the F1 progeny were intercrossed to generate a new line of *Klrc1*$^{-/-}$ mice. Males from the F2 generation were then infected f.p. with 1000 PFU ECTV-Moscow and survival (**A**), body weight (**B**), and blood genome loads (**C**) were measured as described.

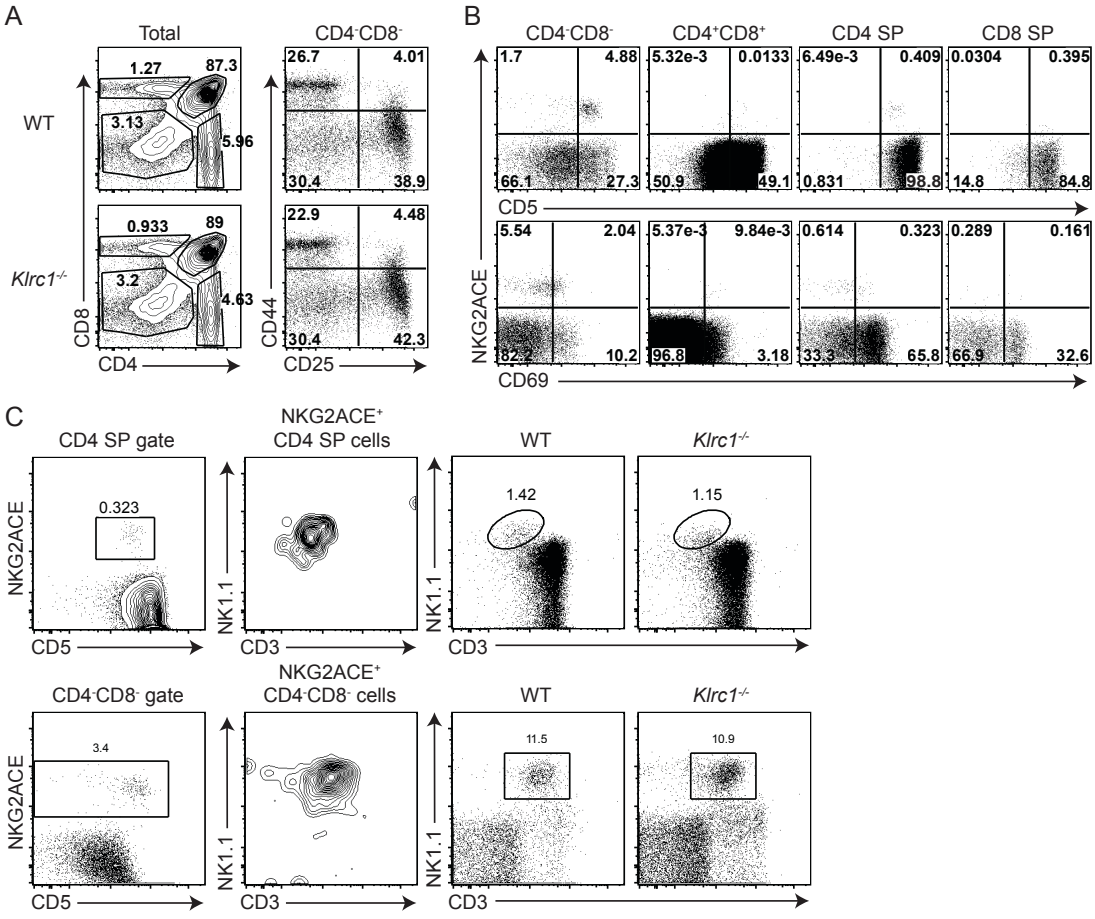

Supplemental Figure 3, related to Figure 3: Normal thymocyte development in *Klrc1*$^{-/-}$ mice. (**A**) Thymuses from WT and *Klrc1*$^{-/-}$ mice were isolated and assessed for overall thymocyte development (left panels). CD4^{-}CD8^{-} thymocytes were then subdivided into DN1-4 subsets by CD44 and CD25 expression (right panels). (**B**) NKG2ACE expression was analyzed on WT thymocytes. (**C**) NKG2ACE^{+} CD4 single-positive (top row) and CD4^{-}CD8^{-} (bottom row) thymocytes from WT thymuses were assessed for NK1.1 and CD3 expression (left two columns) and those population frequencies were then compared in WT and *Klrc1*$^{-/-}$ thymuses (right two columns).

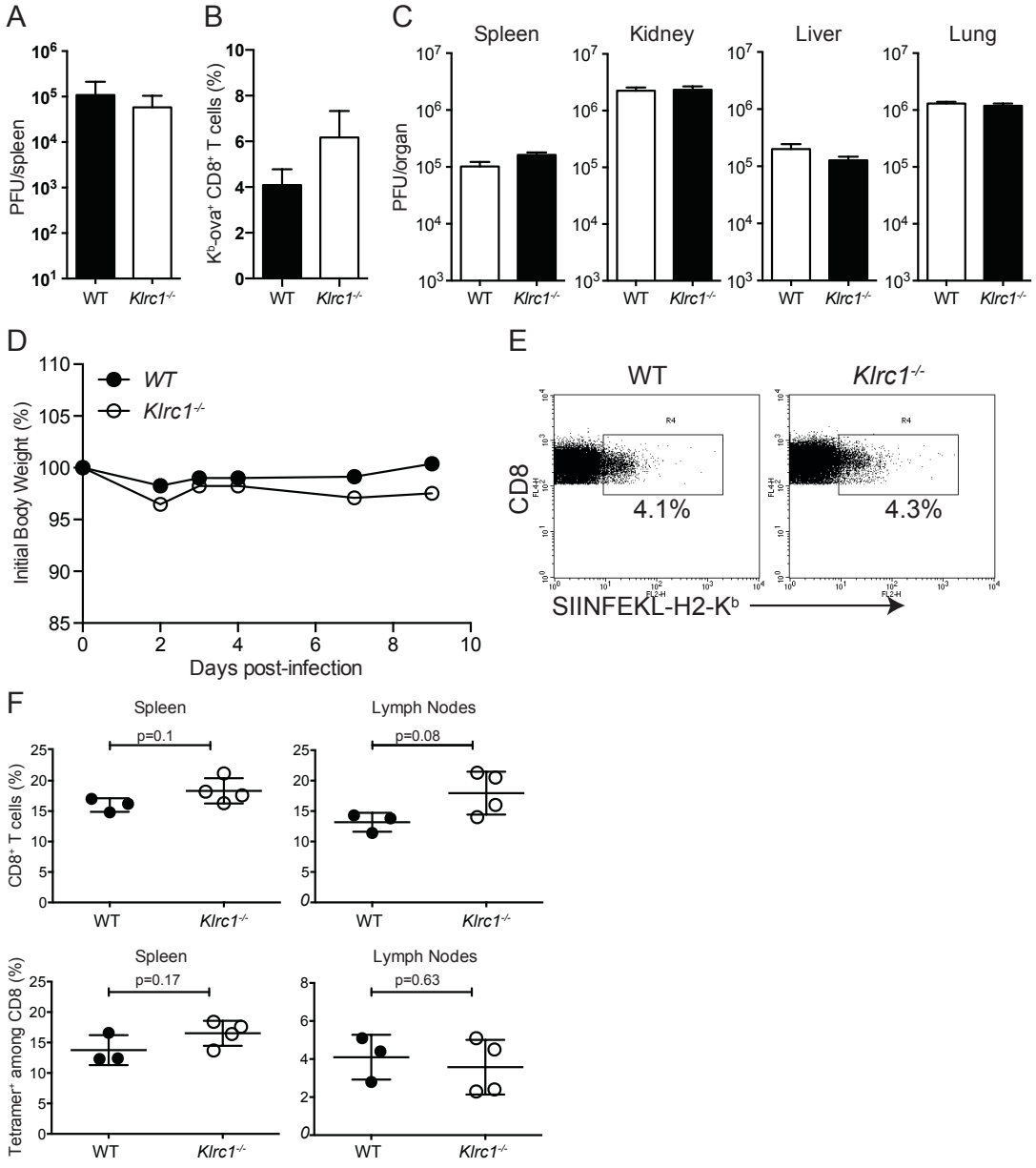

Supplemental Figure 4, related to Figure 6: NKG2A is dispensible for the immune response to VSV, LCMV, and vaccinia virus. (**A, B**) WT and *Klrc1*$^{-/-}$ mice were infected i.v. with 5x10^6 PFU of VSV-ova. Splenic viral burden at 8 hrs p.i. was measured by plaque assay (A). Ova-specific CD8$^+$ T responses were measured by K^b-ova tetramer staining of splenocytes 7 days p.i. (B). (**C**) Mice were infected i.v. with 2x10^6 PFU LCMV clone 13 and viral load was measured in spleen, liver, kidney, and lung tissue at 15 days p.i. by plaque assay. (**D-F**) Mice were infected f.p. with 1.25x10^7 PFU recombinant VV (VV-NP-S-GFP). Body weights were measured out to 9 d.p.i. (D). Frequencies of ova-specific CD8$^+$ T cells were measured by SIINFEKL-K^b tetramer staining at day 9 (E). Frequencies of total CD8$^+$ T cells were quantified from spleens and popliteal

lymph nodes at day 9 (F, top panels). Frequencies of specific $CD8^+$ T cells were quantified from spleens and popliteal lymph nodes at day 9 (F, bottom panels).

Mutation	Location
Point	2749
Deletion	2059 to 2152
Deletion	1888 to 1937
Deletion	-428 to 1559
Point	-749
Point	-1134
Point	-1300
Point	-1455
Point	-1623
Point	-2197
Point	-3720
Point	-3817
Point	-4451
Point	-4466
Point	-4579

Supplemental Table 1, related to Figures 1 and 2: The *Klrc1* locus of the *Klrc1*$^{-/-}$ strain remains essentially intact after targeting. Mutations found within the *Klrc1*$^{-/-}$ locus are shown according to their position relative to the *Klrc1* transcriptional start site. Briefly, WT and *Klrc1*$^{-/-}$ genomic DNA was fragmented and enriched for *Klrc* locus-specific fragments by BAC Capture. Enriched DNA was then cloned into a library, amplified, purified, and subjected to high-throughput sequencing. Alignments were analyzed with Tablet software.

Supplemental Experimental Procedures

Flow cytometry. Spleens and popliteal lymph nodes were digested in collagenase D for 45 min at 37°C and passed through a 70μm mesh filter. Cell suspensions were Fc-blocked in a supernatant containing anti-CD16/CD32 for 15 minutes on ice, then surface-stained with antibodies or tetramers for 20 minutes on ice. For intracellular staining of IFN-γ and CD107a, surface-stained cells were fixed in 2% PFA, then permeabilized and stained according to manufacturer's instructions (BD Cytofix/Cytoperm kit, BD Biosciences). CD3-FITC, CD8-PE, CD8-eFluor450, NK1.1-PerCP.Cy5.5, NKG2A/C/E-biotinylated, NKG2A^{B6}-PE, NKG2A/C/E-FITC, Ly49H-APC, CD11b-PE.Cy7, CD19-PE, CD25-FITC, CD45.1-PE, CD45.2-FITC, CD27-FITC, Ly49all-biotinylated, Ly6C-APC, KLRG1-APC, and CD127-eFluor450 antibodies were obtained from eBioscience. CD94-biotin, SIINFEKL-K^b-PE, NKG2D-PE, and Ly6G-FITC antibodies were obtained from BioLegend. CD5-PE, CD11c-FITC, CD44-PE, CD86-PE, CD49b-PE, CD69-PE, IFN-γ-Alexa647, IFN-γ-PE, CD107a-FITC, TNF-APC, and GMCSF-PE antibodies were obtained from BD Biosciences. Streptavidin-APC was obtained from BD Biosciences. Tetramers for the poxvirus immunodominant B8R$_{20-27}$ epitope (TSYKFESV-H2-K^b) were produced by the NIH Tetramer Core Facility. Ag-specific CD8$^+$ T cells in mice infected with VSV-ova were detected with H-2K^b OVA$_{257-264}$ peptide tetramers (Beckman Coulter). Antigen-specific CD8$^+$ T cells in mice infected with LCMV clone 13 were detected with H-2D^b gp33 peptide tetramers (MBL).

Differential blood cell counts and staining of tissue sections

Blood from ECTV-infected mice was collected 6 to 7 days p.i. by heart-stick directly into EDTA-containing tubes. Complete blood counts and WBC differentials were quantified by the Washington University Medical Center's Division of Comparative Medicine. Spleens, livers, lungs, and kidneys were harvested 6 days p.i. into 10% buffered formalin, stored for 24 hrs at 4°C, transferred to 70% ethanol for 24 to 48 hrs, paraffin-embedded, sectioned, and subjected to H&E staining.

BAC capture and sequencing of the *Klrc* locus. Multiplexed Paired-End Sequencing libraries were made using one microgram of WT or *Klrc1*$^{-/-}$ mouse genomic DNA according to Illumina protocol. 500 to 800 micrograms of 450-bp Adaptor-Modified DNA Fragments were obtained after 14 cycles of PCR amplification. Libraries indexed individually were pooled together in order to obtain one microgram of total DNA. BAC RP23-145F22 (186kb) spanning the *Klre1* to *Klri2* region was used to capture the *Klrc* region. One hundred nanograms of biotinylated BAC DNA were hybridized for 72 hours to the denatured pooled Illumina libraries for which repeat sequences were blocked using mouse cot-1 DNA (Bashiardes et al, 2005). After hybridization, biotinylated BAC fragments were captured using 100 microliters of streptavidin-coated magnetic beads (Invitrogen) and washed using SDS/SSC solutions. Recovered DNA was amplified 12 more cycles using Illumina flow cell specific primers (F5: AATGATACGGCGACCACCGA and R7: CAAGCAGAAGACGGCATACGA).

PCR products were purified using Agencourt AMPure XP beads and quantified with a Qubit 2.0 Fluorometer (life Technology). Fragments were sequenced on HiSeq 2500 instrument (Illumina, San Diego, CA) using 50 bp single-end sequencing option. Reads in Fasta format were aligned to the BAC RP23-145F22 sequence using Bowtie-0.12.7 with the following options –t –v 2 –a –best –m 1 –q. Alignments were visualized using Tablet (Milne et al, 2013).

NK cell activation assay. Splenocytes from ECTV-infected mice were incubated for 6 hours at 37°C with anti-CD107a antibody, in the presence or absence of $1x10^5$ YAC-1 target cells. Brefeldin A and monensin were added for the final 5 hours of the incubation. Cells were then surface stained with anti-NK1.1 and anti-CD3 antibodies, fixed, permeabilized, stained intracellularly with anti-IFN-γ and analyzed by flow cytometry.

$CD8^+$ T cell enrichment and adoptive transfer. To evaluate T cell-intrinsic mechanisms, CD45.1 WT and CD45.2 *Klrc1*$^{-/-}$ mice were challenged with $1x10^3$ to $5x10^3$ PFU ECTV-ova. $CD8^+$ T cells from infected mice were enriched from spleens by magnetic beads (MACS cell separation, Miltenyi Biotec), counted and assessed for specific (B8R-K^{b+}) tetramer staining by flow-cytometry. A 1:1 mix of CD45.1/CD45.2 B8R-$K^{b+}CD8^+$ T cells ($2.5x10^4$ from each strain) was co-transferred into *Rag1*$^{-/-}$ host mice. The hosts were infected in the footpad with $1x10^3$ PFU WT-ECTV the next day. The frequency and numbers of donor cells present in *Rag1*$^{-/-}$ host spleens were assessed 7 days later. To evaluate T cell-

extrinsic mechanisms, approximately $1x10^5$ $B8R^+CD45.1^+$ WT cells were transferred alone into either $CD45.2^+$ WT or $CD45.2^+$ *Klrc1*$^{-/-}$ hosts. Hosts were infected with WT-ECTV the next day and donor specific $CD8^+$ T cell numbers were quantified from host spleens 7 days p.i.

NK cell depletion. At day -2, mice were injected i.p. with 100ul anti-NK1.1-containing ascites, or as a control, injected i.p. with 100μg purified rat IgG (Sigma). On day 0, mice were infected f.p. with 200 PFU ECTV-Moscow. At day 6 or 8, mice were sacrificed and spleens were assayed for antigen-specific $CD8^+$ T cell number by H2-K^b-TSYKFESV tetramer staining. In some experiments, mice were sacrificed at day 0 to assess NK cell depletion by $CD3^-NKp46^+$ staining of splenocytes. Mice treated with anti-NK1.1 consistently showed depletion greater than 80% (data not shown).

Microarray analyses of $CD8^+$ T cell populations. RNA samples were amplified using the Nugen Ovation Pico SL system and labeled with the Nugen Encore Biotin kit. Prepared, labeled cDNA was then hybridized to Mouse Gene 1.0 ST microarray chips (Affymetrix). Principal Component Analysis (PCA) plots were generated using Population PCA software (Harvard Medical School). Individual normalized expression values were visualized with MultiPlot Studio (Broad Institute). Genes with a fluorescence intensity of >120 were considered expressed above background. Differential expression of genes was visualized on volcano plots and significance between sample groups was highlighted if both

$p < 0.05$ and fold change was greater than 1.5-fold in either direction. Heatmaps and hierarchical clustering of relevant genes were generated with GENE-E software (Broad Institute). Gene ontology pathway analysis of ECTV-specific $CD8^+$ T cells was done using DAVID Bioinformatics Database (NIAID). Pathway analysis was considered significant if $p < 0.01$ and at least 5 nonredundant, differentially expressed genes were represented within the pathway.

RT-PCR primer sequences. The following primer sequences were obtained from PrimerBank (Massachusetts General Hospital) and manufactured by Integrated DNA Technologies for use in quantitative RT-PCR reactions: *bim* (F: CCCGGAGATACGGATTGCAC, R: GCCTCGCGGTAATCATTTGC), *batf3* (F: CAGAGCCCCAAGGACGATG, R: GCACAAAGTTCATAGGACACAGC), *tnfaip3* (also known as A20, F: GAACAGCGATCAGGCCAGG, R: GGACAGTTGGGTGTCTCACATT), *Il10* (F: GCTCTTACTGACTGGCATGAG, R: CGCAGCTCTAGGAGCATGTG), *Il10ra* (F: CCCATTCCTCGTCACGATCTC, R: TCAGACTGGTTTGGGATAGGTTT), and *smad3* (F: CACGCAGAACGTGAACACC, R: GGCAGTAGATAACGTGAGGGA).

Supplemental References

Bashiardes S., Veile R., Helms C., Mardis E.R., Bowcock A.M., and Lovett M. (2005) Direct Genomic Selection. Nat. Methods 2, 63-69.

Milne I., Stephen G., Bayer M., Cock P.J., Pritchard L., Cardie L., Shaw P.D., and Marshall D. (2013) Using Tablet for visual exploration of second-generation sequencing data. Brief Bioinform. 14, 193-202.